

Forty Years of Air Temperature Change over Iran Reveals Linear and Nonlinear Warming

Majid KAZEMZADEH¹, Zahra NOORI¹, Sadegh JAMALI^{2*}, and Abdulhakim M. ABDI³

¹ Faculty of Natural Resources, University of Tehran, 77871-31587, Karaj, Iran

² Department of Technology and Society, Lund University, SE-22100, Lund, Sweden

³ Centre for Environmental and Climate Science, Lund University, SE-22362, Lund, Sweden

(Received October 25, 2021; in final form February 1, 2022)

ABSTRACT

Spatiotemporal analysis of long-term changes in air temperature is of prime importance for climate change research and the development of effective mitigation and adaptation strategies. Although there are considerable studies on air temperature change across the globe, most of them have been on linear trends and time series analysis of nonlinear trends have not received enough attention. Here, spatiotemporal patterns of monthly and annual mean (T_{mean}), maximum (T_{max}), and minimum (T_{min}) air temperature at 47 synoptic stations across climate zones in Iran for a 40-yr period (1978–2017) are analyzed. A polynomial fitting scheme (Polytrend) is used to both monthly and annual air temperature data to detect trends and classify them into linear and nonlinear (quadratic and cubic) categories. The significant (non-significant) trends in T_{mean} , T_{max} , and T_{min} across all climate zones are 41.1% (58.9%), 34.1% (65.9%), and 46% (54%), respectively. The highest magnitude of increasing trends is observed in the annual T_{min} ($0.47^{\circ}\text{C decade}^{-1}$) and the lowest magnitude is for the annual T_{max} ($0.4^{\circ}\text{C decade}^{-1}$). Across the country, increasing trends ($\bar{x} = 37.2\%$) have higher spatial coverage than the decreasing trends ($\bar{x} = 3.2\%$). Warming trends in T_{mean} (65.3%) and T_{min} (73.1%) are mainly observed in humid climate zone while warming trends in T_{max} are in semi-arid (43.9%) and arid (34.1%) climates. Linear change with a positive trend is predominant in all T_{mean} (56.7%), T_{max} (67.8%), and T_{min} (71.2%) and for both monthly and annual data. Further, the linear trends have the highest warming rate in annual T_{min} ($0.83^{\circ}\text{C decade}^{-1}$) and T_{mean} ($0.46^{\circ}\text{C decade}^{-1}$) whereas the nonlinear trends have the highest warming rate in annual T_{max} ($0.52^{\circ}\text{C decade}^{-1}$). The linear trend type is predominant across the country especially in humid climate zones whereas the nonlinear trends (quadratic and cubic) are mainly observed in the arid climate zones. This study highlights nonlinear changes and spatiotemporal trends in air temperature in Iran and contributes to a growing body of climate change literature that is necessary for the development of effective mitigation and adaptation strategies in the Middle East.

Key words: linear trends, nonlinear trends, time series analysis, air temperature, Polytrend, Iran

Citation: Kazemzadeh, M., Z. Noori, S. Jamali, et al., 2022: Forty years of air temperature change over Iran reveals linear and nonlinear warming. *J. Meteor. Res.*, **36**(3), 462–477, doi: 10.1007/s13351-022-1184-5.

1. Introduction

The global climate has significantly warmed up over the last 100 years as there has been an average increase of 0.85°C ($0.65\text{--}1.06^{\circ}\text{C}$) in air temperature during 1880–2012 (IPCC, 2013; Shi et al., 2018). This warming is due to increasing concentrations of CO_2 and other greenhouse gases in the atmosphere largely driven by industrialization, land-use change, and use of fossil fuels and biomass (Khattak et al., 2011; Mullick et al., 2019). Air temperature is an important climatic variable that affects human health, natural ecosystems, plant and animal communities, energy–water balance, and the hydrologic

cycle (Kousari et al., 2013; Sonali and Kumar, 2013; Bilbao et al., 2019). Higher temperatures increase evapotranspiration and subsequently atmospheric water vapor content, which can influence surface energy fluxes (Held and Soden, 2000; Dai, 2006; Zhang et al., 2013; Wang et al., 2017; Abdi et al., 2019). Air temperature extremes such as maximum and minimum, warming rates, and their spatial patterns change at both local and regional scales (Yang et al., 2020). There is thus growing concern about the effect of climate change on social and natural systems at those scales (Del Río et al., 2011).

The use of average values (T_{mean}) to indicate temperature increase under climate change ignores variations in

*Corresponding author: Sadegh.jamali@tft.lth.se

© The authors [2022]. This article is published with open access at link.springer.com

local climate and the effects of relocation of stations over time (Li et al., 2004; You et al., 2014). Several studies have pointed out that the rate of change in maximum (T_{\max}) and minimum temperature (T_{\min}) is higher than T_{mean} (Matiu et al., 2016; El Kenawy et al., 2019). Spatiotemporal variations in air temperature present a unique window to understand the complex nonlinear climate system under global warming (Yu et al., 2019). This is particularly relevant in drylands, which cover about 45% of the earth's land surface (Práválie, 2016), as increasing aridity in these regions causes substantial shifts in ecosystem structure and function (Berdugo et al., 2020). In southwest Asia, large swaths of arid and semi-arid land are hotspots for climate change (Tabari and Willems, 2018) as models project future temperatures to exceed human habitability (Pal and Eltahir, 2016).

Iran is the second-largest country in the Middle East. It has a diverse climate varying from very humid montane to coastal hyper-arid, but mostly comprises arid and semi-arid regions (Khalili and Rahimi, 2018). It is also the third-most populous country in the region with 84 million inhabitants (United Nations, 2019). Iran has been experiencing high climatic variability that can change the trend and magnitude of meteorological variables such as temperature, evaporation, and radiation (Moghim, 2018). Therefore, extreme climate events such as heat waves (Perkins-Kirkpatrick and Gibson, 2017; Aboubakri et al., 2019) and droughts (Keshavarz et al., 2013) have severe implications on lives and livelihoods in this country.

Several studies have reported increasing trends in temperature over Iran along with a decrease in rainfall over the last 50 years (Rahimzadeh et al., 2009; Tabari and Talaee, 2011; Nazaripour and Daneshvar, 2014; Ghasemi, 2015; Malekian and Kazemzadeh, 2016). The impact of this climatic change has affected social and natural systems across the country. For example, most lakes in Iran are drying and the dry lakebeds cause sand and dust storms to form (Rashki et al., 2013). These in turn have negative impacts on human health and ecosystems (Najafi et al., 2014; Moghim, 2018). There is a need for research that sheds light on complex nonlinear patterns of important climatic variables, such as air temperature in order to develop effective mitigation and adaptation strategies.

Several studies on temperature trend analysis for Iran have been conducted (Ghasemi and Khalili, 2006; Tabari and Talaee, 2011; Saboohi et al., 2012; Kousari et al., 2013; Ghasemi, 2015; Balling et al., 2016; Soltani et al., 2016; Kazemzadeh and Malekian, 2018; Pour et al., 2019; Doulabian et al., 2021). Most of these studies are concerned with detecting or estimating linear trends

(negative or positive) using ordinary least-squares (OLS) linear regression models. Furthermore, the trend analysis has focused on the magnitude of the trend's slope to address the question of how much the temperature trend increased or decreased in any particular study period. The trend estimation methods chosen in these studies to determine trend direction and magnitude are either parametric, such as student's *t*-test, or non-parametric such as the Mann–Kendall trend test (Mann, 1945; Kendall, 1948).

Long-term changes in climatic variables such as temperature are not always linear and using traditional methods such as linear regression ignores their nonlinear and nonstationary attributes (Ji et al., 2014). These hidden attributes require more advanced methods that reveal their exact nature and identify the cause of change. Here, linear and nonlinear patterns and trends in air temperature time series in the different climate zones of Iran over the last four decades (1978–2017) are analyzed. To do this, a polynomial fitting-based scheme called Polytrend, developed by Jamali et al. (2014), was applied to time series of the monthly and annual mean (T_{mean}), maximum (T_{\max}), and minimum (T_{\min}) air temperature across Iran. The outputs of the analysis include trend types and trend direction and enable the detection of spatiotemporal patterns of temperature over four decades in the country's climate zones.

2. Materials and methods

2.1 Study area

Iran is located in the southwest of Asia and situated over $25^{\circ}00'N$ – $38^{\circ}39'N$, and $44^{\circ}00'$ – $63^{\circ}25'E$ (Fig. 1). According to the Extended De Martonne's climate zone classification (Khalili, 1992), the hyper-arid, arid, semi-arid, Mediterranean, and other humid climate zones cover the 46.1%, 24.5%, 22.9%, 3.2%, and 3.3% of Iran, respectively (Rahimi et al., 2013). Thus, the semi-arid and arid climate zones cover most parts of the country, which are primarily characterized by low rainfall and high potential evapotranspiration. The northern coastal and western parts of Iran have a humid climate while the east and southeast regions are arid and hyper-arid (Fig. 1). Mean annual precipitation is 250 mm yr^{-1} (Eslamian et al., 2009) and temperature extremes vary between -20 and $+50^{\circ}\text{C}$ (Saboohi et al., 2012). Iran has two main mountain ranges, Alborz in the north and Zagros in the west, and their altitudes range from -26 to 5671 m above mean sea level. This topography plays a substantial role in the climate of Iran, due to the fact that they affect the temporal and spatial distribution of temperature, water vapor,

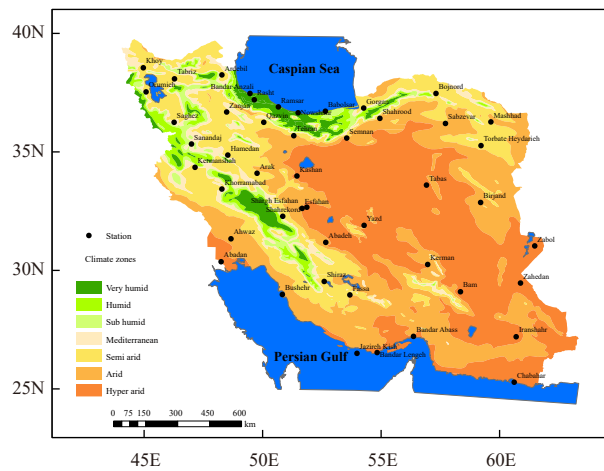


Fig. 1. Synoptic station distribution in the different climate zones of Iran (Khalili, 1992; Rahimi et al., 2013).

and precipitation over the country.

2.2 Data type and source

In the current study, 47 synoptic stations are selected that have uniform coverage across the country and are well-distributed across all climate zones (Fig. 1 and Table 1). These stations are chosen out of more than 200 stations over Iran because they had sufficient and accurate long-term data for the country. The monthly meteorological data are acquired from the Islamic Republic of Iran Meteorological Organization (IRIMO) for a 40-yr period 1978–2017. Here, both monthly (January to December) and annual T_{mean} , T_{max} , and T_{min} covering the 1833 time

series ($3 \times 12 \times 47 = 1692$ monthly and $3 \times 47 = 141$ annual) are used.

2.3 Methods

2.3.1 Data preprocessing

T_{mean} , T_{max} , and T_{min} time series are used because change in T_{mean} can be due to changes in T_{min} or T_{max} , or due to changes in both (Del Río et al., 2007; Tabari and Talaee, 2011; Ahmadi et al., 2018). Monthly data, separately for each month of the year are analyzed because using the composition of some months as a seasonal temperature time series (e.g., combinations such as December, January, and February for winter, etc.) may not show intra-seasonal trends. For some cases, missing data in the monthly time series (e.g., a missing month in a year) are estimated by using the average of the preceding and succeeding months. The normality of the data is verified using the Kolmogorov–Smirnov test (Kolmogorov, 1933; Smirnoff, 1939), and then Polytrend is applied to the verified time series.

2.3.2 Trend detection and classification

Polytrend was applied to the monthly and annual time series to analyze trends in air temperature. Polytrend was developed by Jamali et al. (2014) for trend classification and the specification of linear and nonlinear patterns in time series data. The method consists of a three-phase stage for detecting linear and nonlinear trends and classifying nonlinear trends into quadratic, cubic, and concealed trend types (Fig. 2). A concealed trend is nonlinear and possesses either a cubic or quadratic trend but

Table 1. Characteristics of the synoptic stations and their climate zones used in this study

Station name	Longitude (E)	Latitude (N)	Climate zone	Station name	Longitude (E)	Latitude (N)	Climate zone
Abadan	48°25'	30°37'	Arid	Khorramabad	48°28'	33° 43'	Semi-arid
Abadeh	52°67'	31°18'	Arid	Khoy	44°97'	38° 55'	Semi-arid
Arak	49°77'	34°10'	Semi-arid	Mashhad	59°63'	36° 27'	Sub-arid
Ahwaz	48°67'	31°33'	Arid	Nowshahr	51°50'	36° 65'	Very-humid
Ardeabil	48°28'	38°25'	Semi-arid	Orumieh	45°08'	37° 53'	Semi-arid
Bandar Abass	56°37'	27°22'	Arid	Ramsar	50°67'	36° 90'	Very-humid
Bandar Lengeh	54°83'	26°53'	Hyper-arid	Rasht	49°65'	37°20'	Very-humid
Bandar Anzali	49°47'	37°47'	Humid	Saghez	46°27'	36°25'	Mediterranean
Bushehr	50°83'	28°98'	Arid	Sanandaj	47°00'	35°33'	Semi-arid
Bam	58°35'	29°10'	Hyper-arid	Semnan	53°55'	35°58'	Arid
Birjand	59°20'	32°87'	Arid	Sabzevar	57°72'	36°20'	Arid
Bojnord	57°32'	37°47'	Semi-arid	Shahrood	54°95'	36°42'	Arid
Babol Sar	52°65'	36°72'	Humid	Shahrekord	50°85'	32°28'	Semi-arid
Chabahar	60°62'	25°28'	Hyper-arid	Shiraz	52°60'	29°53'	Semi-arid
Esfahan	51°67'	32°62'	Arid	Shargh Esfahan	51°87'	32°67'	Hyper-arid
Fassa	53°68'	28°97'	Semi-arid	Torbate Heydarieh	59°22'	35°27'	Semi-arid
Qazvin	50°05'	36°25'	Semi-arid	Tabriz	46°28'	38°08'	Semi-arid
Gorgan	54°27'	36°85'	Sub-humid	Tehran	51°32'	35°65'	Arid
Hamedan	48°53'	34°87'	Semi-arid	Tabas	56°92'	33°60'	Arid
Iran shahr	60°70'	27°20'	Hyper-arid	Yazd	54°28'	31°90'	Arid
Jazireh Kish	53°98'	26°50'	Hyper-arid	Zabol	61°48'	31°03'	Arid
Kerman	56°97'	30°25'	Arid	Zanjan	48°48'	36°68'	Semi-arid
Kashan	51°45'	33°98'	Arid	Zahedan	60°88'	29°47'	Hyper-arid
Kermanshah	47°15'	34°35'	Semi-arid				

without net change in temperature from the beginning to the end of the time series. The procedure starts by evaluating the suitability of fitting a cubic polynomial model (highest order polynomial is tested), testing the statistical significance of the fit (in which the a coefficient in $ax^3 + bx^2 + cx + d$ passes a t -test at $\alpha = 0.05$), and by examining the presence of two opposite bends (both a local minimum and maximum) in the polynomial fitted model. Then, a first-order polynomial model is fitted. If all these criteria are met for the fitting of the cubic model and the linear slope is statistically significant (a in the expression $ax + b$), a cubic trend type is assigned. If at least one of these tests fails, the procedure jumps to the quadratic model, the next lower phase. A similar procedure is applied for the presence and testing the significance of a quadratic trend, except that only one bend (maximum or minimum) is sought. The temperature time series is assigned to the concealed trend category if the linear coefficient is not statistically significant for time series with a valid cubic or quadratic trend type. If all tests fail, in the third phase, the suitability of a linear trend type is evaluated through the fitting of a linear model to the monthly and annual temperature time series. A linear trend type is assigned if the linear trend slope is statistically significant. Time series with neither nonlinear nor linear signifi-

cant trends are classified into a no-trend class. For more details, refer to [Jamali et al. \(2014\)](#). In the temperature time series, linear changes are constant over time but nonlinear changes are not constant and can show inter-decadal variation during the study period.

2.3.3 Sensitivity of trend types to climate zones

The climate zone map of Iran proposed by Khalili is used to explore the relationship between climates zones of Iran with detected air temperature trend types and patterns. This climate classification includes seven climate zones: semi-arid, arid, hyper-arid, sub-humid, humid, very-humid, and Mediterranean over Iran ([Fig. 1](#)). Using the climate zones allows for the comparison results for trend direction and trend types in monthly and annual T_{mean} , T_{max} , and T_{min} time series among different climate zones.

3. Results

3.1 Spatial patterns and temporal trends in T_{mean}

Linear, quadratic, and cubic trend types in T_{mean} across Iran are 56.5% (52.6% increasing and 3.9% decreasing), 13.1% (7.9% increasing and 5.2% decreasing), and 30.3% (28.7% increasing and 1.6% decreasing), respectively ([Table 2](#)). [Figure 3](#) shows the distribution of trend signi-

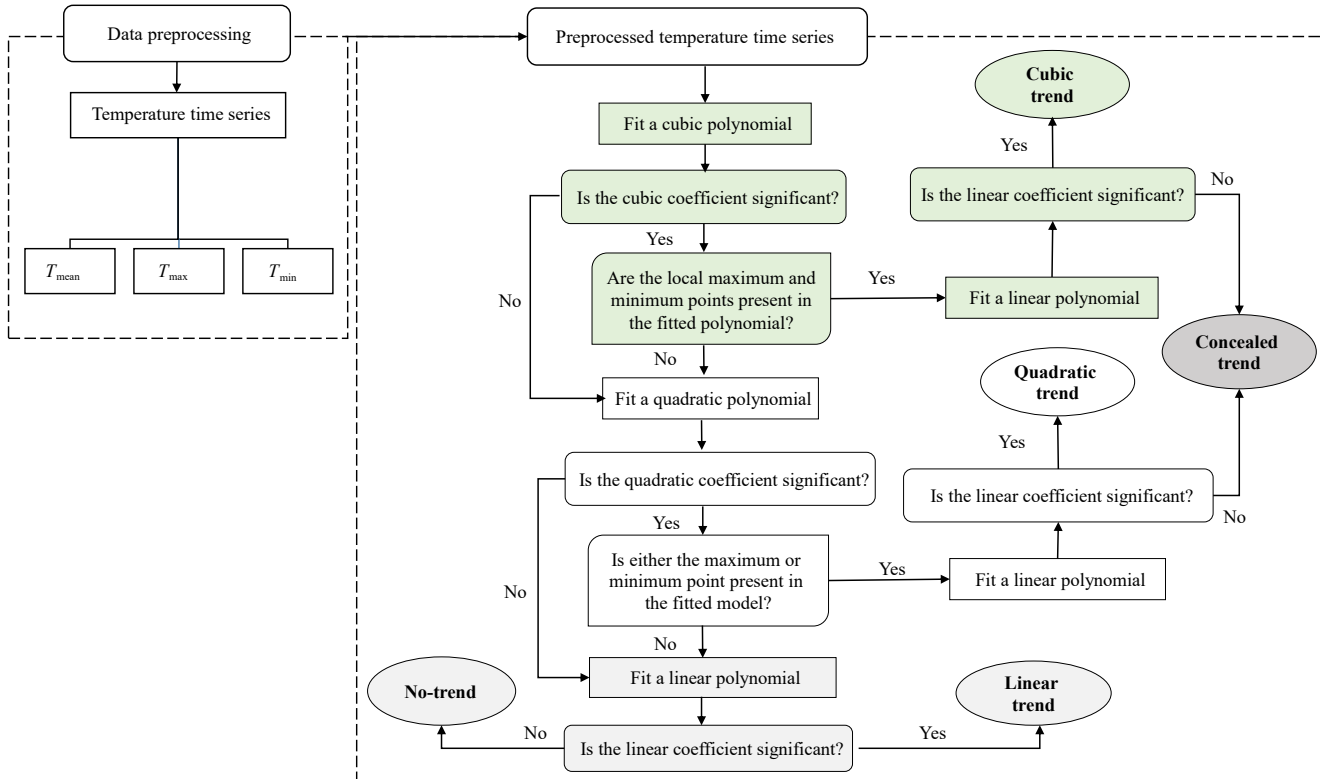


Fig. 2. Flowchart of our methodology for analyzing trends in air temperature using Polytrend ([Jamali et al., 2014](#); shown in the dashed box to the right).

Table 2. Percentage of significant increasing and decreasing trends for the linear and nonlinear classes in monthly and annual T_{mean} at different climate zones ($\alpha = 0.05$)

	Linear		Quadratic		Cubic	
	Increasing	Decreasing	Increasing	Decreasing	Increasing	Decreasing
Hyper-arid	58.3	0.0	2.8	2.8	33.3	2.8
Arid	55.2	4.6	6.9	1.1	32.2	0.0
Semi-arid	41.5	6.1	12.2	4.9	30.5	4.9
Mediterranean	0.0	12.5	0.0	87.5	0.0	0.0
Humid	64.7	0.0	11.8	0.0	23.5	0.0
Sub-humid	100.0	0.0	0.0	0.0	0.0	0.0
Very-humid	83.3	0.0	5.6	0.0	11.1	0.0
Entire country	52.6	3.9	7.9	5.2	28.7	1.6

ficance in monthly and annual T_{mean} (Fig. 3a), the trend direction (Fig. 3b), and trend types (Fig. 3c) detected in different climate zones. The significant and non-significant trends in T_{mean} across all climate zones are 41.1% and 58.9%, respectively. For the significant trends, 36.5% are increasing and 4.6% are decreasing over the studied period. Majority of the significant trends are observed in the humid climate (65.3%) and Mediterranean (61.5%) climat-

ic zones (Fig. 3a). Conversely, lower proportions of the significant trends are in the sub-humid (23.1%) and semi-arid (37.0%) climate zones. Most of the climate zones have an increasing trend except the Mediterranean, which has a decreasing trend (Fig. 3b). The sub-humid and very-humid climate zones have the highest percentage for linear trend type with 100% and 83.3%, respectively. The Mediterranean climate zone has the highest

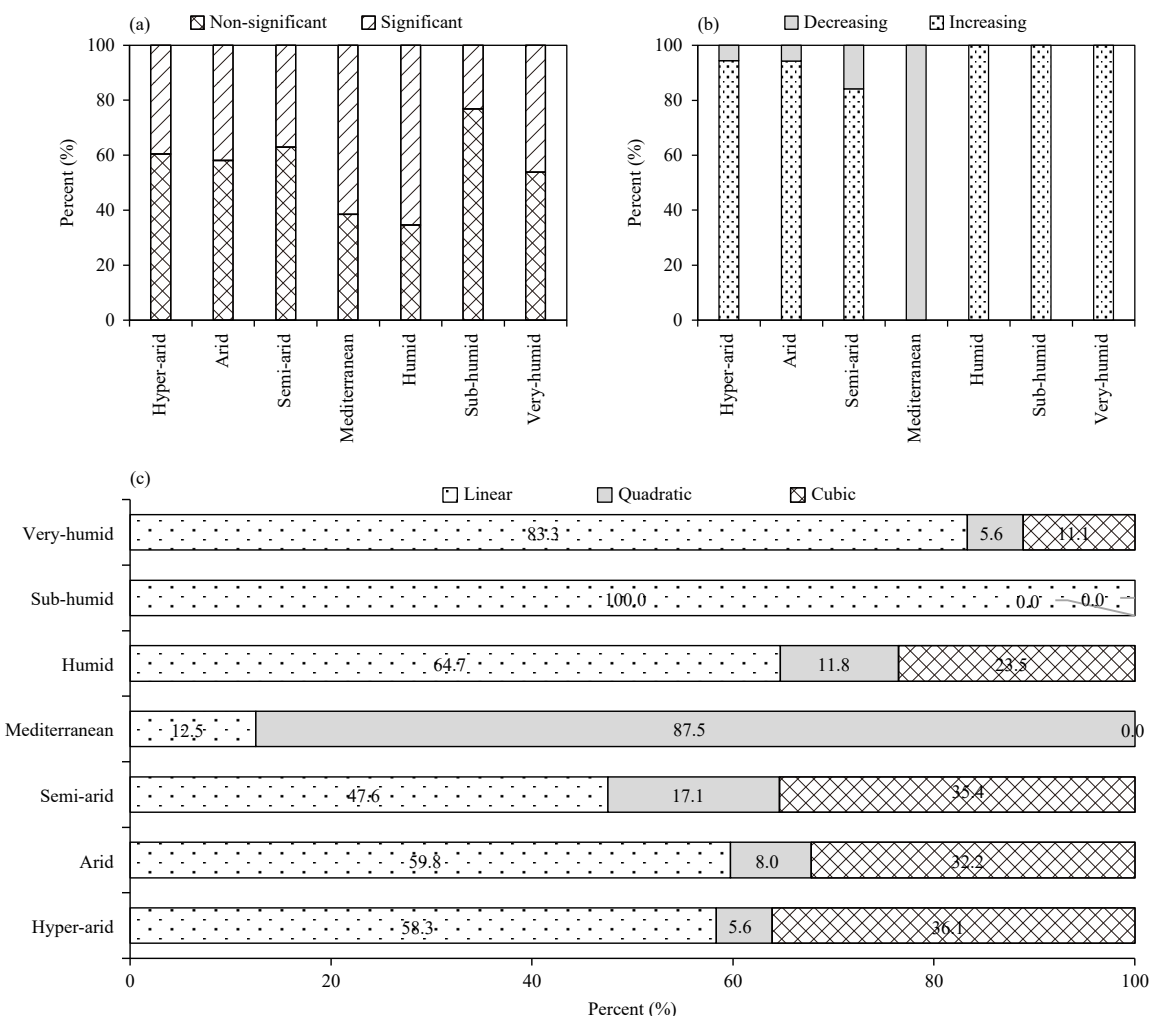


Fig. 3. Distributions of (a) significant and non-significant trends, (b) significant increasing and decreasing trends, and (c) type of trends detected in monthly and annual T_{mean} time series in different climate zones over Iran.

percentage for quadratic type of trends (87.5%) and the least percentage for linear type (12.5%). The majority trend types in the hyper-arid, arid, and semi-arid climate zones are linear and cubic (Fig. 3c and Table 2). Some typical temperature time series (T_{mean}) with detected trend types of cubic, cubic concealed, quadratic, quadratic concealed, linear, and no-trend are depicted in Fig. 4.

Temporal distribution of trend significance, direction, and types detected in monthly and annual time series of T_{mean} (1978–2017) are shown in Fig. 5. The monthly spider chart in Fig. 5a shows that the significant trends are mainly in March (72.3%), May (70.2%), and June

(61.7%), while January (14.9%), April (19.1%), November (19.1%), and December (10.6%) have the least significant change. Furthermore, Fig. 5b shows that all months except November have a significant increasing trend. For the annual data, 63.8% of the detected trends in T_{mean} over the country are significant (59.6% increasing and 4.2% decreasing). With regard to different trend types on a temporal scale, the months with dominant (> 70%) linear trends in T_{mean} are January, May, June, July, November, and December. Conversely, the lowest proportion of linear trends are in February, March, April, and October (Fig. 5c). Dominant type of trend observed

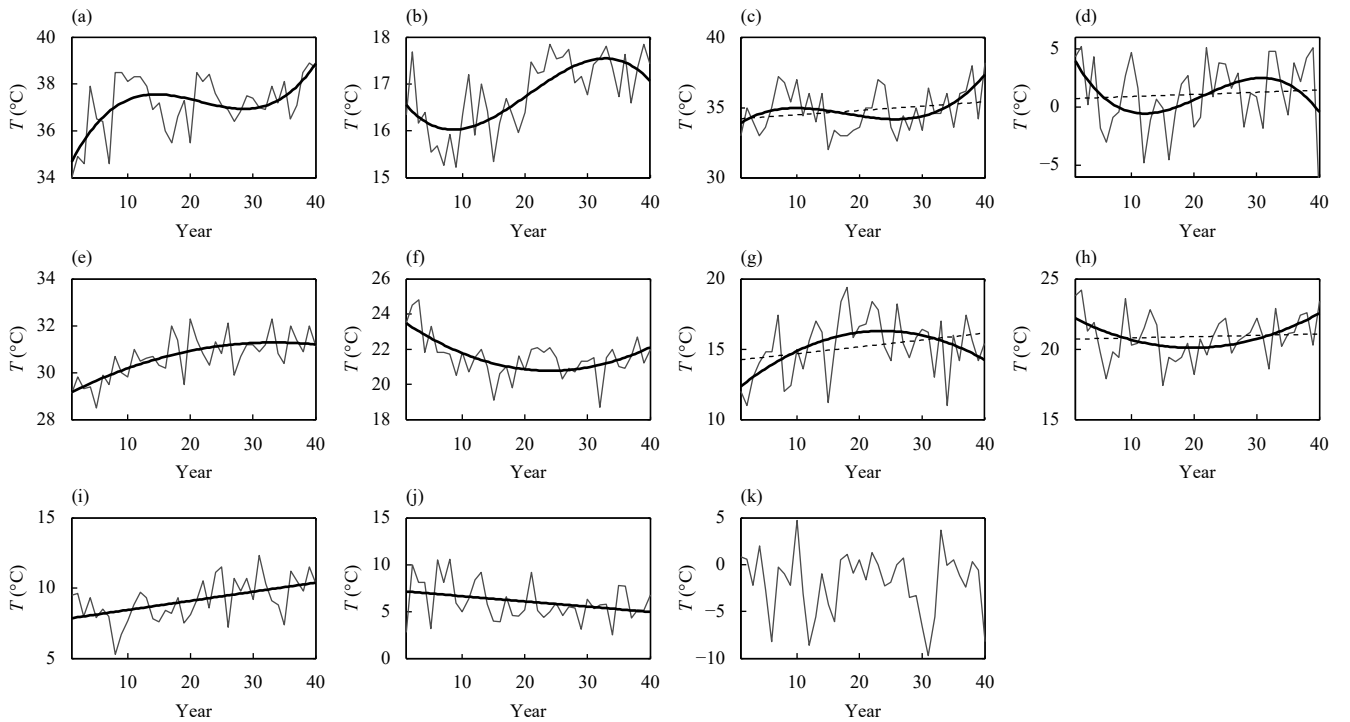


Fig. 4. Typical examples of T_{mean} time series with a detected trend type of (a, b) cubic, (c, d) cubic concealed, (e, f) quadratic, (g, h) quadratic concealed, (i, j) linear, and (k) no-trend. The dashed lines in the concealed trends denote non-significant linear fits.

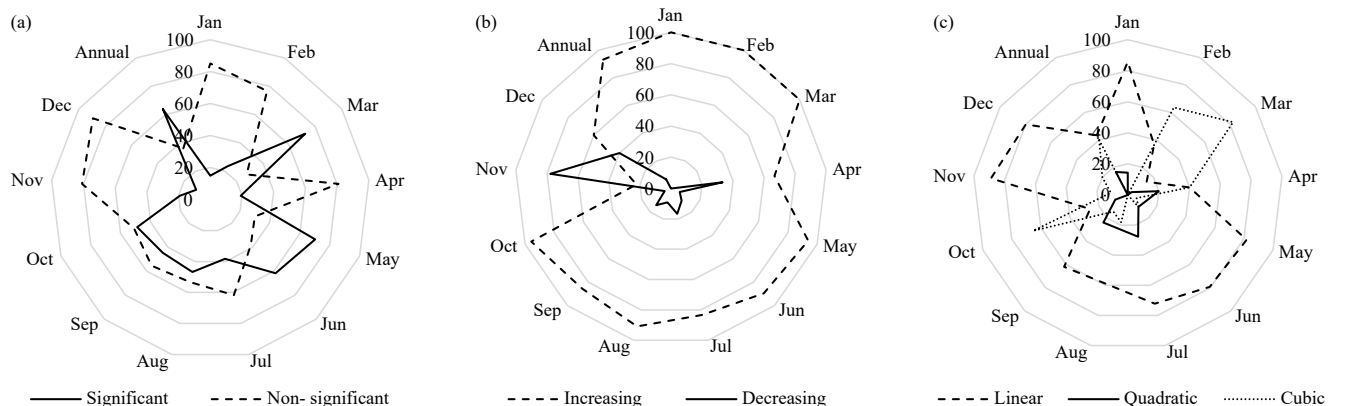


Fig. 5. Temporal distributions of (a) the significant and non-significant trends, (b) significant increasing and decreasing trends, (c) linear, quadratic, and cubic trends in monthly and annual time series of T_{mean} .

in February (63.6%), March (82.3%), and October (65.2%) is cubic, while the quadratic trend type is lower than 30% over the monthly and annual time series. In the annual time series, the proportion of linear, quadratic, and cubic trend types are respectively 43.3% (only increasing), 16.7% (10% increasing and 6.7% decreasing), and 40% (only increasing).

Figure 6 shows significant trend magnitudes of annual T_{mean} ranged from -0.44 to $+0.78^{\circ}\text{C decade}^{-1}$. In average, the magnitude of annual T_{mean} has increased $0.4^{\circ}\text{C decade}^{-1}$ across the country. The highest increasing trend magnitude is in semi-arid climate ($0.45^{\circ}\text{C decade}^{-1}$) while the lowest increasing trend magnitude is detected in very-humid climate ($0.35^{\circ}\text{C decade}^{-1}$). The magnitude of the decreasing trend in annual T_{mean} is the highest in the Mediterranean climate with $-0.44^{\circ}\text{C decade}^{-1}$. Moreover, linear trend type in annual T_{mean} has the highest increasing magnitude ($0.47^{\circ}\text{C decade}^{-1}$) compared to quadratic ($0.33^{\circ}\text{C decade}^{-1}$) and cubic types ($0.35^{\circ}\text{C decade}^{-1}$) (**Fig. 6**).

3.2 Spatial patterns and temporal trends in T_{max}

Distributions of trend significance, direction, and type in monthly and annual T_{max} time series for different climate zones are shown in **Fig. 7**. Of the trends detected in monthly and annual T_{max} time series, 34.1% are significant (32.6% increasing and 1.5% decreasing). The majority of these are in semi-arid (43.9%) and arid (34.1%) climate zones, while the Mediterranean does not show any significant trend (**Fig. 7a**). Distribution of direction of the significant trends indicates that all of the climate zones except the hyper-arid zone have more than 97% increasing trends in T_{max} (**Fig. 7b**).

As with T_{mean} , the coverage of linear trends in T_{max}

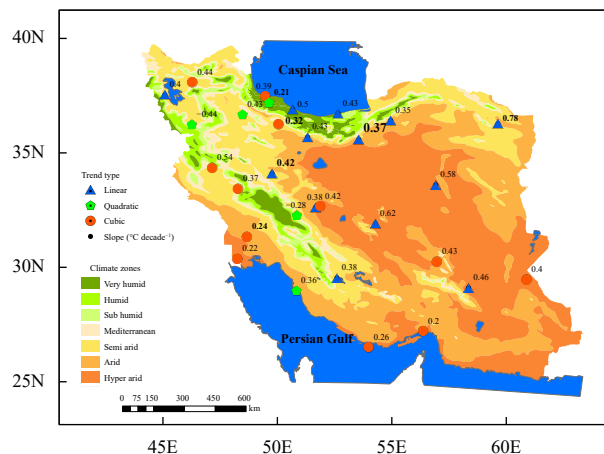


Fig. 6. Distribution of significant trend types and trend magnitude (slope) in annual time series of T_{mean} .

with 67.8% (66.8% increasing and 1% decreasing) is more than that for nonlinear quadratic 12.9% (12.5% increasing and 1.4% decreasing) and cubic 18.2% (16.3% increasing and 1.9% decreasing) (**Table 3**). Regarding spatial distribution of trend types per climate zone, linear trends dominate the humid (100%), very-humid (84%), and sub-humid (75%) climate zones (**Fig. 7c**). The cubic trend type is present in hyper-arid, arid, and semi-arid ($\bar{x} = \sim 22\%$) and the quadratic type is in all climate zones except humid and the Mediterranean ($\bar{x} = 18\%$). Overall, T_{max} shows higher proportions of increasing linear trend types compared to nonlinear cubic and quadratic trends across all climate zones (**Fig. 7c** and **Table 3**).

The spider charts in **Fig. 8** show the temporal distributions of trend significance, direction, and type detected in monthly and annual T_{max} time series (1978–2017). More than 50% of significant trends are mostly in February, March, May, and annual data, while non-significant trends are observed in December (**Fig. 8a**). The annual time series of T_{max} shows 72.3% significant trends (70.2% increasing and 2.1% decreasing), and all the monthly time series have increasing trends greater than 85% except November and December (**Fig. 8b**). The winter and spring months have the highest significant increasing trends (January, 100%; February, 100%; and March, 96%) among the monthly and annual T_{max} time series. The trend type classification in the monthly time series reveals that the linear type is the dominant class in almost all months with values greater than 50% except for December and March. Moreover, the cubic class has the highest proportion of trend types in March (67%). In the annual time series, most of the trends are linear 52.9% (increasing), quadratic 26.5% (increasing), and cubic 20.6% (17.6% increasing and 2.9% decreasing) (**Fig. 8c**).

The magnitude of significant trends detected in the annual T_{max} across Iran varied from -0.66 to $+0.72^{\circ}\text{C decade}^{-1}$ with a mean increase of $0.47^{\circ}\text{C decade}^{-1}$ (**Fig. 9**). The semi-arid climate ($0.54^{\circ}\text{C decade}^{-1}$) has the highest increasing trend magnitude relative to other climate zones. Conversely, the magnitude of the decreasing trend is highest in the hyper-arid climate with $-0.66^{\circ}\text{C decade}^{-1}$. In the annual T_{max} data, the cubic trend type has the highest magnitude ($0.52^{\circ}\text{C decade}^{-1}$) compared to linear ($0.47^{\circ}\text{C decade}^{-1}$) and quadratic types ($0.41^{\circ}\text{C decade}^{-1}$), respectively.

3.3 Spatial patterns and temporal trends in T_{min}

Spatial distributions of trend significance, direction, and type in the monthly and annual T_{min} time series for

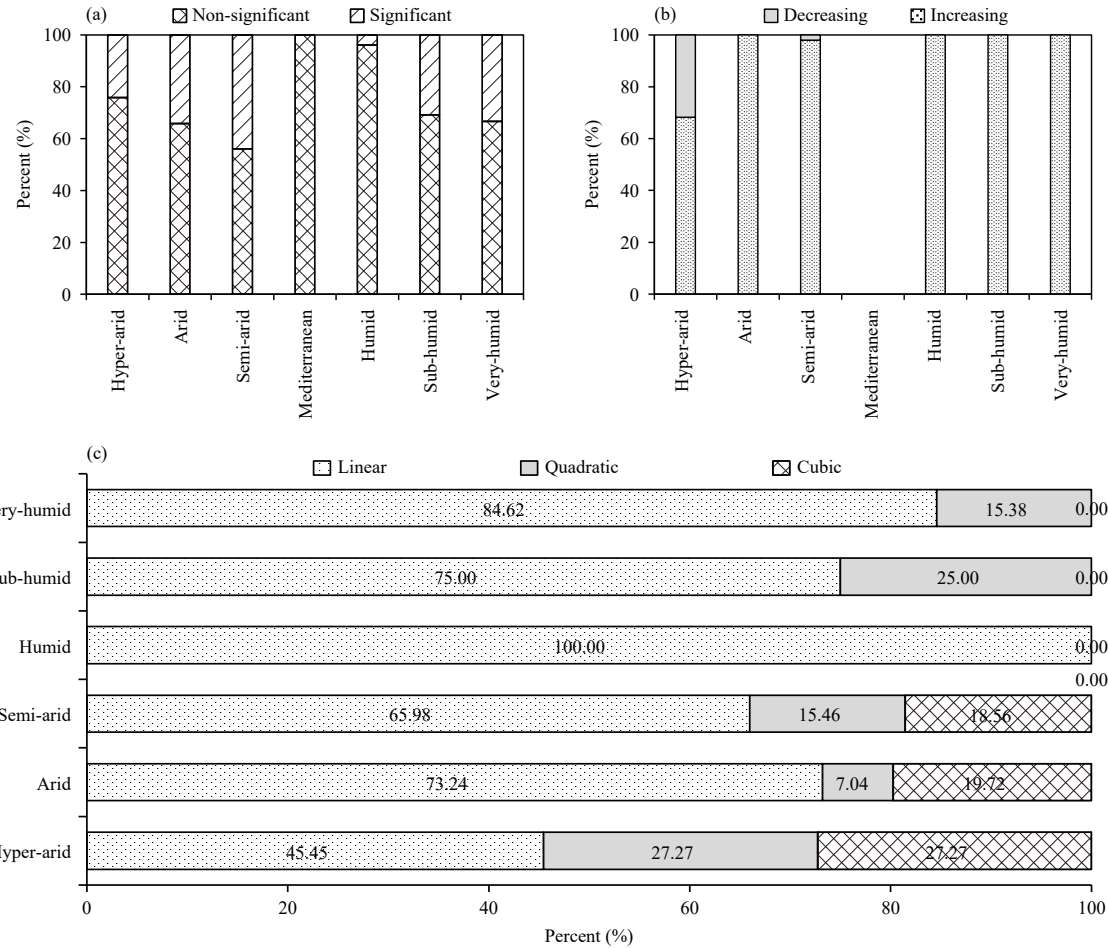


Fig. 7. As in Fig. 3, but for T_{\max} .

Table 3. As in Table 2, but for T_{\max}

	Linear		Quadratic		Cubic	
	Increasing	Decreasing	Increasing	Decreasing	Increasing	Decreasing
Arid	73.2	0.0	7.0	0.0	19.7	0.0
Semi-arid	63.9	2.1	15.5	0.0	18.6	0.0
Hyper-arid	45.5	0.0	13.6	13.6	9.1	18.2
Humid	100.0	0.0	0.0	0.0	0.0	0.0
Mediterranean	0.0	0.0	0.0	0.0	0.0	0.0
Sub-humid	75.0	0.0	25.0	0.0	0.0	0.0
Very-humid	84.6	0.0	15.4	0.0	0.0	0.0
Entire country	66.8	1	12.5	1.4	16.3	1.9

different climate zones are shown in Fig. 10. The trend in monthly and annual T_{\min} time series showed significance in 46% of the data points (42.6% increasing and 3.4% decreasing) over the country (Fig. 10a). The detected trends in T_{\min} are mostly in the hyper-arid (61.5%), humid (73.1%), and very humid (56.4%) climates (Fig. 10a). More than 85% of detected trends in almost all climate zones are increasing except in the Mediterranean and sub-humid climate zones (Fig. 10b).

For all climate zones, 71.1% of the detected trends in T_{\min} are linear (66.5% increasing and 4.6% decreasing),

13.9% are quadratic (11.4% increasing and 2.5% decreasing), and 14.9% are cubic (14.6% increasing and 0.3% decreasing). The sub-humid climate zone has the highest proportion of linear trend (100%) while the Mediterranean has the lowest proportion (40%) (Fig. 10c and Table 4). Meanwhile, the majority of nonlinear (quadratic) trends are in the Mediterranean climate relative to other climates zones (Table 4).

Temporal distributions of trend significance, direction, and type in monthly and annual time series of T_{\min} are given in Fig. 11. The results reveal that most of the signi-

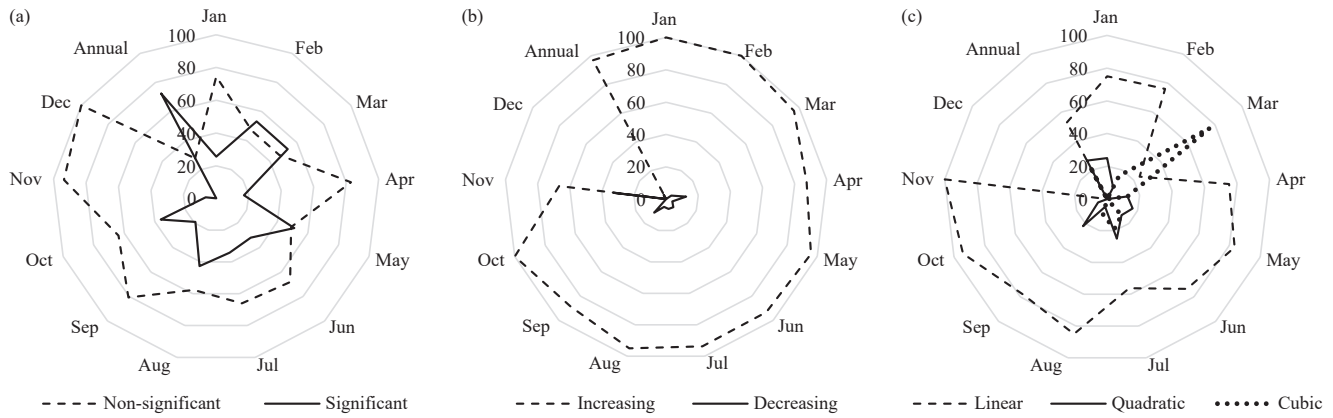


Fig. 8. As in Fig. 5, but for T_{\max} .

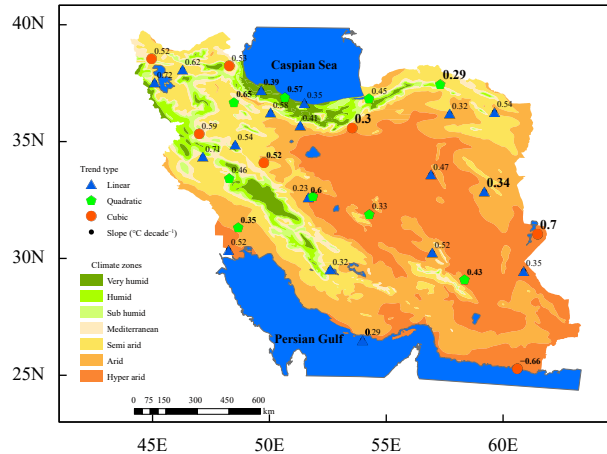


Fig. 9. As in Fig. 6, but for T_{\max} .

fificant trends are in January (78.7%) and June (89.4%) in contrast to February (27.7%), March (17%), May (25.5%), and December (14.8%) with non-significant trends (Fig. 11a). The increasing trends in T_{\min} are in more than 75% of data points in the annual aggregation and across all months except December (Fig. 11b). In addition, the majority of increasing trends in T_{\min} are observed in the spring and summer months rather than autumn and winter. For the annual T_{\min} time series, 17% (12.7% increasing and 4.3% decreasing) of the observed trends are significant over the country (Fig. 11b).

With regard to different trend types detected in T_{\min} , almost all months and the annual time series follow the linear trend type except March and December that show cubic and quadratic trends, respectively. In the T_{\min} annual time series, we only find the linear trend type with 100% (75% increasing and 25% decreasing) (Fig. 11c). The dominant trend types detected in March (50%) and December (42.9%) are cubic and quadratic, respectively (Fig. 11c).

Figure 12 shows the magnitude of trends in annual

T_{\min} varying from -0.55 to $+1.19^{\circ}\text{C decade}^{-1}$ with a mean increase of $0.47^{\circ}\text{C decade}^{-1}$. The hyper-arid climate has the highest increasing trend magnitude with $0.95^{\circ}\text{C decade}^{-1}$. In contrast, the magnitude of the decreasing trend is highest in the sub-humid climate with $-0.69^{\circ}\text{C decade}^{-1}$. As mentioned above, the annual T_{\min} has only linear trend type with increasing and decreasing magnitudes of 0.83 and $-0.62^{\circ}\text{C decade}^{-1}$, respectively (Fig. 12).

4. Discussion

4.1 Trends in T_{mean} , T_{\max} , and T_{\min}

Our findings indicate that T_{\min} has the largest relative proportion of significant trends across the country followed by T_{mean} and T_{\max} . The proportion of increasing trends is also found to be greatest for T_{\min} and least for T_{\max} . The highest magnitude of increasing trends is observed in the annual T_{\min} ($0.47^{\circ}\text{C decade}^{-1}$) and the lowest magnitude is for the annual T_{\max} ($0.4^{\circ}\text{C decade}^{-1}$). Across the country, increasing trends ($\bar{x} = 37.2\%$) have higher spatial coverage than the decreasing trends ($\bar{x} = 3.2\%$). Our findings are in agreement with Soltani et al. (2016), Tabari and Talaee (2011), and Duhan et al. (2013), which increasing trends in T_{\min} over Iran were higher than T_{\max} . They suggested that the warming trend of T_{mean} in Iran occurred mostly due to the increase in T_{\min} rather than T_{\max} during the past decades. Wang et al. (2018) found a similar pattern over China where T_{\min} warmed at a higher magnitude than T_{\max} in the recent decades. This could confirm the greenhouse gas effects or aerosols on the raised T_{\min} by changing longwave radiation fluxes (Stjern et al., 2020). The increase in T_{\min} may be linked to polluted and saturated air in the early morning (Tabari and Talaee, 2011) resulting from temperature inversion and stable weather conditions in industrialized regions (Türkes et al., 1996; Bani-Domi,

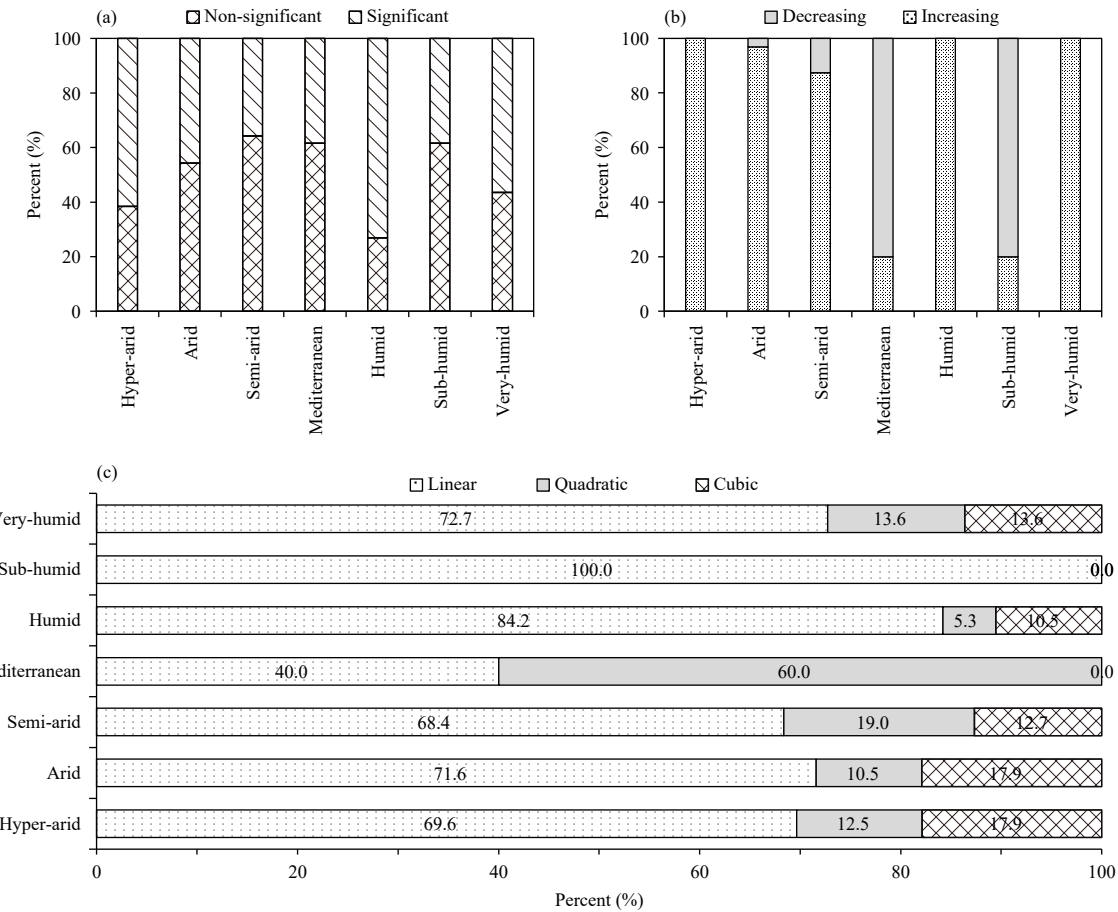


Fig. 10. As in Fig. 3, but for T_{\min} .

Table 4. As in Table 2, but for T_{\min}

Climate zones	Linear		Quadratic		Cubic	
	Increasing	Decreasing	Increasing	Decreasing	Increasing	Decreasing
Hyper-arid	0.0	69.6	0.0	12.5	0.0	17.9
Arid	3.2	68.4	0.0	10.5	0.0	17.9
Semi-arid	6.3	62.0	5.1	13.9	1.3	11.4
Mediterranean	20.0	20.0	60.0	0.0	0.0	0.0
Humid	0.0	84.2	0.0	5.3	0.0	10.5
Sub-humid	80.0	20.0	0.0	0.0	0.0	0.0
Very-humid	0.0	72.7	0.0	13.6	0.0	13.6
Entire country	4.6	66.5	2.5	11.4	14.6	0.3

2005; Tabari and Talaee, 2011). As Iran is rapidly developing, land-use change can also contribute to increases in both T_{\max} and T_{\min} due to urbanization, industrialization, land conversion, and land abandonment (Kousari et al., 2013; Qiu et al., 2016). Land-use can change the temperature of the land surface, and as a result, influence air temperature as the two are tightly coupled (Gallo et al., 2011).

Climate change leads to increased temperature variability and change in temperature extremes such as T_{\max} and T_{\min} (IPCC, 2013; Ma et al., 2015), while T_{mean} increases gradually in response (Matiu et al., 2016). Some earlier studies only investigated one variable of temperat-

ure time series (i.e., T_{mean} , T_{\max} , or T_{\min}). For example, Ageena et al. (2013) reported significant warming in T_{\min} over the last 32 years in Libya. Our analysis of the three temperature variables indicates that they have changed asymmetrically over the past four decades.

4.2 Spatial patterns

Areas with warming trends in annual T_{mean} are mainly located in the north and northwestern parts of Iran. While the majority of stations located in the central and northeastern corner of the country have more increasing trends in annual T_{\max} instead. These findings are consistent with the results of Saboohi et al. (2012) and Fallah-Ghalhari et

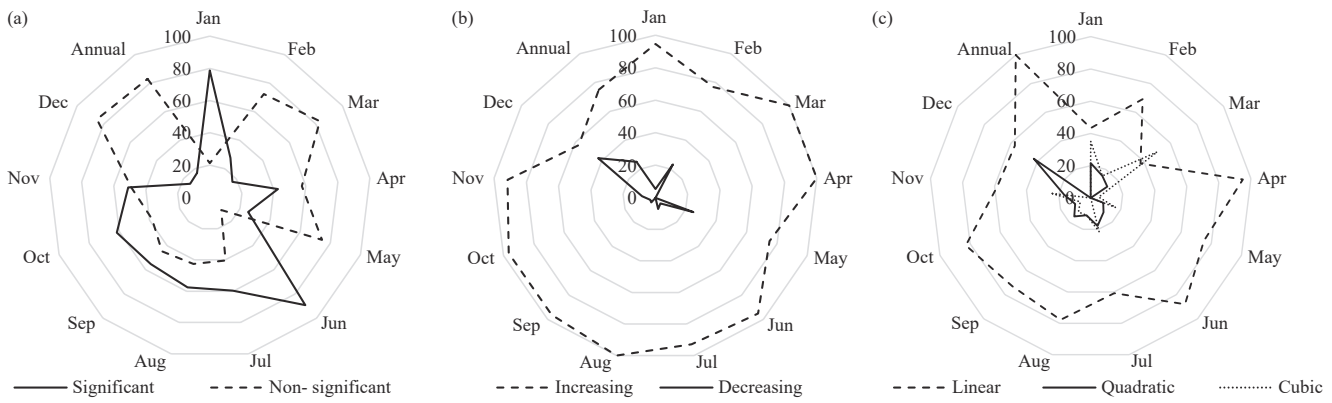


Fig. 11. As in Fig. 5, but for T_{\min} .

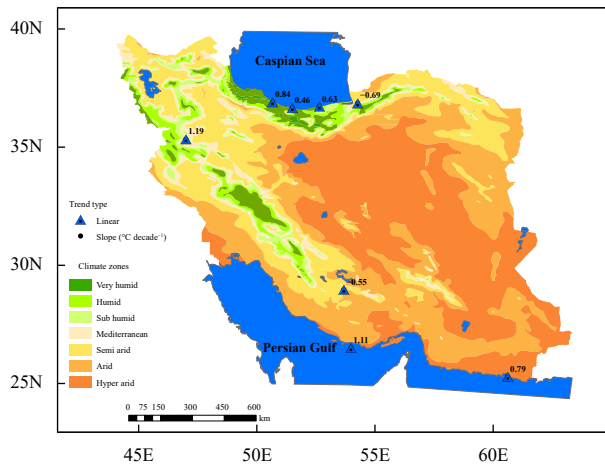


Fig. 12. As in Fig. 6, but for T_{\min} .

al. (2019) that reported western and northwestern parts of Iran experienced significant warming trends. Most of the regions located along the southern Caspian Sea coast have experienced positive trends in all annual T_{mean} , T_{\max} , and T_{\min} time series. This indicates that the lowlands with warmer climates, such as central and eastern regions, are warming at a higher rate than mountainous regions with colder climates that are mostly situated in western and northwestern parts of the country. These results echo the findings of Tabari and Talaee (2011), Kousari et al. (2013), and Ghasemi (2015) that Iranian lowlands are warming faster than the highlands. Uncertainties in distinguishing the effects of anthropogenic and natural factors on temperature change hinder robust identification of the response of the temperature to different forcings (IPCC, 2018). There are reports of no detectable spatial pattern in the temperature trend over Iran (Ghahraman, 2006; Saboohi et al., 2012; Kousari et al., 2013). However, this could be due a result of simple trend detection methods that do not take into consideration the temporal nonlinearity of the trends.

4.3 Temporal trends

At monthly scale, our findings indicate that the increasing trends in T_{mean} and T_{\max} are mainly in March and May, while they exhibit the least significant trends in November and December. In T_{\min} , the highest proportion of increasing significant trends is in January and June while the lowest proportion is in December. Here, in general, the monthly T_{mean} and T_{\max} time series indicate that the increasing trends are mainly in spring months whereas decreasing trends are in the autumn months. However, using T_{\min} time series, we find increasing trends mainly in the spring and summer months rather than the autumn and winter months. This is in line with the finding of Ghasemi (2015) who demonstrated that warming trends over Iran occurred mostly in summer and spring than winter and autumn. Also, Daneshvar et al. (2019) revealed that minimum and maximum temperatures over Iran mostly increased in summer periods. Similarly, Cohen et al. (2012) reported increasing global air temperature trends across all seasons apart from winter and that this phenomenon is seasonal. Extreme temperature increases over Iran in the spring could have a significant impact on the irrigated crop yields in the growing season. Studies have reported that an increase in springtime temperature negatively affects tillering and germination and led to the loss of wheat yield (Soureshjani et al., 2019).

Our results are in agreement with Ahmadi et al. (2018) who found that 62% of all stations in Iran experienced an increasing trend in annual temperature between 1961 and 2010. Another analysis, by Saboohi et al. (2012), of annual T_{mean} , T_{\max} , and T_{\min} time series between 1951 and 2007 produced significant trends in 71%, 66%, and 40% of their stations, respectively. However, in contrast to our findings, they specified that the significant increasing trends of T_{mean} and T_{\max} were much more than T_{\min} . Importantly, the magnitude of increasing trends in annual temperature time series was higher than decreasing ones.

This means that almost all the significant temperature trends over Iran have been increasing over the last 40 years. This is in agreement with other studies that have analyzed trends at regional, continental, and global scales (Qu et al., 2014; Dashkhuu et al., 2015; Matiu et al., 2016; Mohorji et al., 2017; Rahmstorf et al., 2017; Yu et al., 2019).

4.4 Climate zones

Regarding the magnitude and direction of the trends detected in the different climate zones, our findings indicate that there is an increasing trend in the T_{mean} , T_{max} , and T_{min} time series in almost all climate zones except the Mediterranean zone, which mainly have decreasing trends. Tabari and Talaee (2011), Kousari et al. (2013), and Ahmadi et al. (2018) reported that the temperature had warming trends over the country except for some stations (Saghez and Shahrekord stations) with decreasing trends located in the Mediterranean climate zone. The majority of the significant trends are found for T_{mean} and T_{min} in humid zone, followed by the areas that showed more significant trends of T_{max} located in semi-arid and arid zones. Based on the climate zones in the country, north and northwestern Iran have the humid climate. Thus, significant changes in T_{min} are in agreement with the findings of Fathian et al. (2020) that reported that higher warming in T_{min} was observed in north and northwestern Iran. In contrast, mostly non-significant trends for T_{mean} and T_{max} were evident in the Mediterranean zone and for T_{min} in the semi-arid climate zone. The strongest warming trends in annual T_{mean} and T_{max} were more conspicuous in semi-arid climates with 0.45 and $0.54^{\circ}\text{C decade}^{-1}$, respectively. Karandish et al. (2017) reported similar results for Iran and the highest warming in annual T_{max} were observed in semi-arid climatic zones. While for annual T_{min} , the hyper-arid climate zone had the highest increasing trend magnitude with $0.95^{\circ}\text{C decade}^{-1}$. Essentially, annual T_{min} has the strongest warming in hyper-arid and very-humid climate zones compared to other climate zones. Furthermore, our findings of trend detection were aligned with Geng et al. (2016) who reported the temperature variables (T_{mean} , T_{max} , and T_{min}) have significant warming trends in arid areas of China. Additionally, the strong warming trends observed in annual T_{mean} and T_{max} in semi-arid climate are consistent with the finding of Huang et al. (2012) who reported the enhanced global semi-arid warming implies drier and warmer trends for these regions. Generally, all temperature variables have increased during the last 40 years, but the rate of this warming is asymmetry in the different climates and regions (Karl et al., 1993;

Cox et al., 2020).

4.5 Linear and nonlinear trends

Most of the temperature time series have a greater proportion of linear change ($\bar{x} = 65.1\%$) compared to nonlinear change ($\bar{x} = 17.2\%$) across Iran. This is probably because global air temperature response is near-linear to cumulative atmospheric CO₂ emissions (Collins et al., 2013; Leduc et al., 2015). Importantly, our findings reveal that the linear trends are mostly in humid, sub-humid, and very-humid climate zones, and nonlinear trends are mainly in the Mediterranean, hyper-arid, semi-arid, and arid climate zones. It is clear that air temperature series in arid climates are highly variable due to the low amount of humidity and precipitation and with higher interannual variability. In contrast, air temperature in the humid climate is less varied relative to the arid climate zone. This could explain the linear changes observed in the temperature time series in the humid climate, particularly in northern and western parts of Iran. Moreover, the high temperature variability in the arid zone may cause nonlinear changes in this region. In moisture-limited regions, increased warming is linked to drying and reduction in the latent heat relative to sensible heat (King, 2019). This is due to the fact that soil moisture limits latent heat flux in these regions (Gentine et al., 2007) and changes in moisture availability alter the balance of energy fluxes leading to nonlinearities.

One of the most important reasons for the linear and gradual increase observed in temperature time series is suburban land use change such as conversion of agricultural areas to residential zones within the different climate zones of Iran. Land use change is generally a slow process and does not cause an abrupt change in the temperature time series (Ghahraman, 2006) leading to nonlinear trend behavior. Moreover, linear and nonlinear changes may be associated with several other phenomena over the country such as Arctic Oscillation (Ghasemi and Khalili, 2006; Saboohi et al., 2012), the El Niño–Southerm Oscillation (Pour et al., 2019), increased concentrations of anthropogenic greenhouse gases, aerosols, and cloud cover (Smadi, 2006; Feizi et al., 2014), rapid industrialization, and land use change (Khattak et al., 2011; Mullick et al., 2019).

The highest rates of warming are in linear changes of annual T_{mean} ($0.46^{\circ}\text{C decade}^{-1}$) and T_{min} ($0.83^{\circ}\text{C decade}^{-1}$) over the country. In contrast, the highest rate of warming in annual T_{max} is detected in cubic type with $0.52^{\circ}\text{C decade}^{-1}$. Thus, linear trend type in annual T_{min} demonstrate a higher magnitude compared to annual T_{mean} and T_{max} . The results indicate that the temperature

response to warming is linear in most parts of the country but some areas have experienced nonlinear warming changes, especially for T_{\max} . The drivers of local nonlinear changes (quadratic and cubic) may be due to the changes in other atmospheric variables (King et al., 2018), surface snow/ice cover, and evapotranspiration (Good et al., 2015), changes in anthropogenic aerosols (King et al., 2018), land cover/land use change, and total cloudiness (El Kenawy et al., 2019). Good et al. (2015) have also demonstrated nonlinearities in warming at regional and local scales that are associated with accelerated atmospheric CO₂ concentration over more lands locations on the globe. However, it seems that changing air temperature linearly and nonlinearly resulted from a combination of atmospheric and land system factors.

4.6 Limitations

Although the temperature data of ground-based synoptic stations can be defined as a high-quality dataset in the country, there are limitations and uncertainties about extending station-based results across a large country such as Iran. The sparse spatial distribution of stations in some regions of the country is a limitation in our study. Spatially aggregated temperature datasets are generally preferred in order to decrease uncertainties in station-based time series. Importantly, the methodology employed here does not consider breakpoints in temperature time series, and nonlinear changes seem to be prone to having abrupt changes and breakpoints. Thus, considering abrupt changes in nonlinear trends may provide more detailed information on breakpoints within temperature data that could signify important biophysical processes.

5. Conclusions

A polynomial fitting scheme (Polytrend) is applied for monthly and annual mean (T_{mean}), maximum (T_{\max}), and minimum (T_{\min}) air temperatures time series over Iran for the last 40 years (1978–2017). In addition to detecting trends, Polytrend can classify them into classes of linear and nonlinear (quadratic and cubic) types. The significant (non-significant) trends in T_{mean} , T_{\max} , and T_{\min} across all climate zones are 41.1% (58.9%), 34.1% (65.9%), and 46% (54%), respectively. The results indicate that air temperature has considerably increased over Iran during the last 40 years and that the linear trend type is predominant across the country. Linear trends have the highest warming rate in annual T_{\min} ($0.83^{\circ}\text{C decade}^{-1}$) and T_{mean} ($0.46^{\circ}\text{C decade}^{-1}$) whereas nonlinear trends have the highest warming rate in annual T_{\max} ($0.52^{\circ}\text{C decade}^{-1}$). The majority of linear trends are observed in more hu-

mid zones while nonlinear trends (quadratic and cubic) are mainly detected in more arid zones. Furthermore, our results indicate that air temperature has changed linearly rather than nonlinearly during 1978–2017. Polytrend provides more comprehensive information about the trend (i.e., direction, magnitude, types, and linear/nonlinear patterns) in the monthly and annual data series. Finally, due to fact that the Polytrend provides additional information about trend types and patterns, this methodology is suggested for application to future trends studies.

Acknowledgments. The authors would like to thank the Islamic Republic of Iran Meteorological Organization (IRIMO) for providing the synoptic temperature data. Abdulhakim M. Abdi was supported by the Swedish Research Council (2018-00430).

REFERENCES

- Abdi, A. M., N. Boke-Olén, H. Jin, et al., 2019: First assessment of the plant phenology index (PPI) for estimating gross primary productivity in African semi-arid ecosystems. *Int. J. Appl. Earth Obs. Geoinformation*, **78**, 249–260, doi: [10.1016/j.jag.2019.01.018](https://doi.org/10.1016/j.jag.2019.01.018).
- Aboubakri, O., N. Khanjani, Y. Jahani, et al., 2019: The impact of heat waves on mortality and years of life lost in a dry region of Iran (Kerman) during 2005–2017. *Int. J. Biometeorol.*, **63**, 1139–1149, doi: [10.1007/s00484-019-01726-w](https://doi.org/10.1007/s00484-019-01726-w).
- Ageena, I., N. Macdonald, and A. P. Morse, 2013: Variability of minimum temperature across Libya (1945–2009). *Int. J. Climatol.*, **33**, 641–653, doi: [10.1002/joc.3452](https://doi.org/10.1002/joc.3452).
- Ahmadi, F., M. N. Tahroudi, R. Mirabbasi, et al., 2018: Spatiotemporal trend and abrupt change analysis of temperature in Iran. *Meteor. Appl.*, **25**, 314–321, doi: [10.1002/met.1694](https://doi.org/10.1002/met.1694).
- Balling, R. C. Jr., M. S. K. Kiani, and S. S. Roy, 2016: Anthropogenic signals in Iranian extreme temperature indices. *Atmos. Res.*, **169**, 96–101, doi: [10.1016/j.atmosres.2015.09.030](https://doi.org/10.1016/j.atmosres.2015.09.030).
- Bani-Domi, M., 2005: Trend analysis of temperatures and precipitation in Jordan. Ph.D. dissertation, Dept. of Geography, Yarmouk University, Irbid-Jordan, 100 pp.
- Berdugo, M., M. Delgado-Baquerizo, S. Soliveres, et al., 2020: Global ecosystem thresholds driven by aridity. *Science*, **367**, 787–790, doi: [10.1126/science.aay5958](https://doi.org/10.1126/science.aay5958).
- Bilbao, J., R. Román, and A. De Miguel, 2019: Temporal and spatial variability in surface air temperature and diurnal temperature range in Spain over the period 1950–2011. *Climate*, **7**, 16, doi: [10.3390/cli7010016](https://doi.org/10.3390/cli7010016).
- Cohen, J. L., J. C. Furtado, M. Barlow, et al., 2012: Asymmetric seasonal temperature trends. *Geophys. Res. Lett.*, **39**, L04705, doi: [10.1029/2011GL050582](https://doi.org/10.1029/2011GL050582).
- Collins, M., R. Knutti, J. L. Arblaster, et al., 2013: Long-term climate change: Projections, commitments and irreversibility. *Climate Change 2013: The Physical Science Basis. Contribution of Working Group I to the Fifth Assessment Report of the Intergovernmental Panel on Climate Change*, T. F. Stocker, D. Qin, G.-K. Plattner, et al., Eds., Cambridge University Press, Cambridge, 1029–1136.

- Cox, D. T. C., I. M. D. Maclean, A. S. Gardner, et al., 2020: Global variation in diurnal asymmetry in temperature, cloud cover, specific humidity and precipitation and its association with leaf area index. *Glob. Change Biol.*, **26**, 7099–7111, doi: [10.1111/gcb.15336](https://doi.org/10.1111/gcb.15336).
- Dai, A. G., 2006: Recent climatology, variability, and trends in global surface humidity. *J. Climate*, **19**, 3589–3606, doi: [10.1175/JCLI3816.1](https://doi.org/10.1175/JCLI3816.1).
- Daneshvar, M. R. M., M. Ebrahimi, and H. Nejadsoleymani, 2019: An overview of climate change in Iran: Facts and statistics. *Environ. Syst. Res.*, **8**, 7, doi: [10.1186/s40068-019-0135-3](https://doi.org/10.1186/s40068-019-0135-3).
- Dashkhuu, D., J. P. Kim, J. A. Chun, et al., 2015: Long-term trends in daily temperature extremes over Mongolia. *Wea. Climate Extremes*, **8**, 26–33, doi: [10.1016/j.wace.2014.11.003](https://doi.org/10.1016/j.wace.2014.11.003).
- Del Río, S., R. Fraile, L. Herrero, et al., 2007: Analysis of recent trends in mean maximum and minimum temperatures in a region of the NW of Spain (Castilla y León). *Theor. Appl. Climatol.*, **90**, 1–12, doi: [10.1007/s00704-006-0278-9](https://doi.org/10.1007/s00704-006-0278-9).
- Del Río, S., L. Herrero, C. Pinto-Gomes, et al., 2011: Spatial analysis of mean temperature trends in Spain over the period 1961–2006. *Glob. Planet. Change*, **78**, 65–75, doi: [10.1016/j.gloplacha.2011.05.012](https://doi.org/10.1016/j.gloplacha.2011.05.012).
- Doulabian, S., S. Golian, A. S. Toosi, et al., 2021: Evaluating the effects of climate change on precipitation and temperature for Iran using RCP scenarios. *J. Water Climate Change*, **12**, 166–184, doi: [10.2166/wcc.2020.114](https://doi.org/10.2166/wcc.2020.114).
- Duhan, D., A. Pandey, K. P. S. Gahalaut, et al., 2013: Spatial and temporal variability in maximum, minimum and mean air temperatures at Madhya Pradesh in central India. *Comptes Rendus Geosci.*, **345**, 3–21, doi: [10.1016/j.crte.2012.10.016](https://doi.org/10.1016/j.crte.2012.10.016).
- El Kenawy, A. M., J. I. Lopez-Moreno, M. F. McCabe, et al., 2019: Daily temperature extremes over Egypt: Spatial patterns, temporal trends, and driving forces. *Atmos. Res.*, **226**, 219–239, doi: [10.1016/j.atmosres.2019.04.030](https://doi.org/10.1016/j.atmosres.2019.04.030).
- Eslamian, S. S., J. Abedi-Koupai, M. J. Amiri, et al., 2009: Estimation of daily reference evapotranspiration using support vector machines and artificial neural networks in greenhouse. *Res. J. Environ. Sci.*, **3**, 439–447, doi: [10.3923/rjes.2009.439.447](https://doi.org/10.3923/rjes.2009.439.447).
- Fallah-Ghalhari, G., F. Shakeri, and A. Dadashi-Roudbari, 2019: Impacts of climate changes on the maximum and minimum temperature in Iran. *Theor. Appl. Climatol.*, **138**, 1539–1562, doi: [10.1007/s00704-019-02906-9](https://doi.org/10.1007/s00704-019-02906-9).
- Fathian, F., M. Ghadami, P. Haghghi, et al., 2020: Assessment of changes in climate extremes of temperature and precipitation over Iran. *Theor. Appl. Climatol.*, **141**, 1119–1133, doi: [10.1007/s00704-020-03269-2](https://doi.org/10.1007/s00704-020-03269-2).
- Feizi, V., M. Mollashahi, M. Frajzadeh, et al., 2014: Spatial and temporal trend analysis of temperature and precipitation in Iran. *Ecopersia*, **2**, 727–742. Available online at <http://ecopersia.modares.ac.ir/article-24-6002-en.html>. Accessed on 30 May 2022.
- Gallo, K., R. Hale, D. Tarpley, et al., 2011: Evaluation of the relationship between air and land surface temperature under clear- and cloudy-sky conditions. *J. Appl. Meteor. Climatol.*, **50**, 767–775, doi: [10.1175/2010JAMC2460.1](https://doi.org/10.1175/2010JAMC2460.1).
- Geng, Q. L., P. T. Wu, and X. N. Zhao, 2016: Spatial and temporal trends in climatic variables in arid areas of Northwest China. *Int. J. Climatol.*, **36**, 4118–4129, doi: [10.1002/joc.4621](https://doi.org/10.1002/joc.4621).
- Gentine, P., D. Entekhabi, A. Chehbouni, et al., 2007: Analysis of evaporative fraction diurnal behaviour. *Agric. For. Meteor.*, **143**, 13–29, doi: [10.1016/j.agrformet.2006.11.002](https://doi.org/10.1016/j.agrformet.2006.11.002).
- Ghahraman, B., 2006: Time trend in the mean annual temperature of Iran. *Turk. J. Agric. For.*, **30**, 439–448. Available online at <https://profdoc.um.ac.ir/paper-abstract-203712.html>. Accessed on 30 May 2022.
- Ghasemi, A. R., 2015: Changes and trends in maximum, minimum and mean temperature series in Iran. *Atmos. Sci. Lett.*, **16**, 366–372, doi: [10.1002/asl2.569](https://doi.org/10.1002/asl2.569).
- Ghasemi, A. R., and D. Khalili, 2006: The influence of the Arctic Oscillation on winter temperatures in Iran. *Theor. Appl. Climatol.*, **85**, 149–164, doi: [10.1007/s00704-005-0186-4](https://doi.org/10.1007/s00704-005-0186-4).
- Good, P., J. A. Lowe, T. Andrews, et al., 2015: Nonlinear regional warming with increasing CO₂ concentrations. *Nat. Climate Change*, **5**, 138–142, doi: [10.1038/nclimate2498](https://doi.org/10.1038/nclimate2498).
- Held, I. M., and B. J. Soden, 2000: Water vapor feedback and global warming. *Annu. Rev. Energy Environ.*, **25**, 441–475, doi: [10.1146/annurev.energy.25.1.441](https://doi.org/10.1146/annurev.energy.25.1.441).
- Huang, J., X. Guan, and F. Ji, 2012: Enhanced cold-season warming in semi-arid regions. *Atmos. Chem. Phys.*, **12**, 5391–5398, doi: [10.5194/acp-12-5391-2012](https://doi.org/10.5194/acp-12-5391-2012).
- IPCC, 2013: *Climate Change 2013: The Physical Science Basis. Contribution of Working Group I to the Fifth Assessment Report of the Intergovernmental Panel on Climate Change*, T. F. Stocker, D. Qin, G.-K. Plattner, et al., Eds., Cambridge University Press, Cambridge, 1535 pp, doi: [10.1017/CBO9781107415324](https://doi.org/10.1017/CBO9781107415324).
- IPCC, 2018: *Summary for policymakers. Global Warming of 1.5°C, An IPCC Special Report on the Impacts of Global Warming of 1.5°C above Pre-industrial Levels and Related Global Greenhouse Gas Emission Pathways, in the Context of Strengthening the Global Response to the Threat of Climate Change, Sustainable Development, and Efforts to Eradicate Poverty*, V. Masson-Delmotte, P. M. Zhai, H.-O. Pörtner, et al., Eds., IPCC, Geneva, 32 pp.
- Jamali, S., J. Seaquist, L. Eklundh, et al., 2014: Automated mapping of vegetation trends with polynomials using NDVI imagery over the Sahel. *Remote Sens. Environ.*, **141**, 79–89, doi: [10.1016/j.rse.2013.10.019](https://doi.org/10.1016/j.rse.2013.10.019).
- Ji, F., Z. H. Wu, J. P. Huang, et al., 2014: Evolution of land surface air temperature trend. *Nat. Climate Change*, **4**, 462–466, doi: [10.1038/nclimate2223](https://doi.org/10.1038/nclimate2223).
- Karandish, F., S. S. Mousavi, and H. Tabari, 2017: Climate change impact on precipitation and cardinal temperatures in different climatic zones in Iran: Analyzing the probable effects on cereal water-use efficiency. *Stoch. Environ. Res. Risk Assess.*, **31**, 2121–2146, doi: [10.1007/s00477-016-1355-y](https://doi.org/10.1007/s00477-016-1355-y).
- Karl, T. R., P. D. Jones, R. W. Knight, et al., 1993: Asymmetric trends of daily maximum and minimum temperature. *Bull. Amer. Meteor. Soc.*, **74**, 1007–1023, doi: [10.1175/1520-0477\(1993\)074<1007:ANPORG>2.0.CO;2](https://doi.org/10.1175/1520-0477(1993)074<1007:ANPORG>2.0.CO;2).
- Kazemzadeh, M., and A. Malekian, 2018: Changeability evaluation of hydro-climate variables in Western Caspian Sea region, Iran. *Environ. Earth Sci.*, **77**, 120, doi: [10.1007/s12665-018-7305-x](https://doi.org/10.1007/s12665-018-7305-x).
- Kendall, M. G., 1948: *Rank Correlation Methods*. 4th Ed., Griffin, London, 160 pp.

- Keshavarz, M., E. Karami, and F. Vanclay, 2013: The social experience of drought in rural Iran. *Land Use Policy*, **30**, 120–129, doi: [10.1016/j.landusepol.2012.03.003](https://doi.org/10.1016/j.landusepol.2012.03.003).
- Khalili, A., 1992: Arid and semi arid regions of Iran. Proceeding of Seminar on the Problems of Iranian Deserts and Kavirs, Yazd, Iran, 566–579.
- Khalili, A., and J. Rahimi, 2018: Climate. *The Soils of Iran*, M. Roozitalab, H. Siadat, and A. Farshad, Eds., Springer, Cham, 19–33.
- Khattak, M. S., M. S. Babel, and M. Sharif, 2011: Hydro-meteorological trends in the upper Indus River basin in Pakistan. *Climate Res.*, **46**, 103–119, doi: [10.3354/cr00957](https://doi.org/10.3354/cr00957).
- King, A. D., 2019: The drivers of nonlinear local temperature change under global warming. *Environ. Res. Lett.*, **14**, 064005, doi: [10.1088/1748-9326/ab1976](https://doi.org/10.1088/1748-9326/ab1976).
- King, A. D., R. Knutti, P. Uhe, et al., 2018: On the linearity of local and regional temperature changes from 1.5°C to 2°C of global warming. *J. Climate*, **31**, 7495–7514, doi: [10.1175/JCLI-D-17-0649.1](https://doi.org/10.1175/JCLI-D-17-0649.1).
- Kolmogorov, A., 1933: Sulla Determinazione Empirica di una Legge di Distribuzione. *Giornale dell'Istituto Italiano degli Attuari*, **4**, 83–91.
- Kousari, M. R., H. Ahani, and R. Hendi-Zadeh, 2013: Temporal and spatial trend detection of maximum air temperature in Iran during 1960–2005. *Glob. Planet. Change*, **111**, 97–110, doi: [10.1016/j.gloplacha.2013.08.011](https://doi.org/10.1016/j.gloplacha.2013.08.011).
- Leduc, M., H. D. Matthews, and R. De Elia, 2015: Quantifying the limits of a linear temperature response to cumulative CO₂ emissions. *J. Climate*, **28**, 9955–9968, doi: [10.1175/JCLI-D-14-00500.1](https://doi.org/10.1175/JCLI-D-14-00500.1).
- Li, Q. X., X. N. Liu, H. Z. Zhang, et al., 2004: Detecting and adjusting temporal inhomogeneity in Chinese mean surface air temperature data. *Adv. Atmos. Sci.*, **21**, 260–268, doi: [10.1007/BF02915712](https://doi.org/10.1007/BF02915712).
- Ma, G., A. A. Hoffmann, and C. S. Ma, 2015: Daily temperature extremes play an important role in predicting thermal effects. *J. Exp. Biol.*, **218**, 2289–2296, doi: [10.1242/jeb.122127](https://doi.org/10.1242/jeb.122127).
- Malekian, A., and M. Kazemzadeh, 2016: Spatio-temporal analysis of regional trends and shift changes of autocorrelated temperature series in Urmia Lake Basin. *Water Resour. Manage.*, **30**, 785–803, doi: [10.1007/s11269-015-1190-9](https://doi.org/10.1007/s11269-015-1190-9).
- Mann, H. B., 1945: Nonparametric tests against trend. *Econometrica*, **13**, 245–259, doi: [10.2307/1907187](https://doi.org/10.2307/1907187).
- Matiu, M., D. P. Ankerst, and A. Menzel, 2016: Asymmetric trends in seasonal temperature variability in instrumental records from ten stations in Switzerland, Germany and the UK from 1864 to 2012. *Int. J. Climatol.*, **36**, 13–27, doi: [10.1002/joc.4326](https://doi.org/10.1002/joc.4326).
- Moghim, S., 2018: Impact of climate variation on hydrometeorology in Iran. *Glob. Planet. Change*, **170**, 93–105, doi: [10.1016/j.gloplacha.2018.08.013](https://doi.org/10.1016/j.gloplacha.2018.08.013).
- Mohorji, A. M., Z. Sen, and M. Almazroui, 2017: Trend analyses revision and global monthly temperature innovative multi-duration analysis. *Earth Syst. Environ.*, **1**, 9 pp, doi: [10.1007/s41748-017-0014-x](https://doi.org/10.1007/s41748-017-0014-x).
- Mullick, M. R. A., R. M. Nur, M. J. Alam, et al., 2019: Observed trends in temperature and rainfall in Bangladesh using pre-whitening approach. *Glob. Planet. Change*, **172**, 104–113, doi: [10.1016/j.gloplacha.2018.10.001](https://doi.org/10.1016/j.gloplacha.2018.10.001).
- Najafi, M. S., F. Khoshakhlagh, S. M. Zamanzadeh, et al., 2014: Characteristics of TSP loads during the Middle East springtime dust storm (MESDS) in Western Iran. *Arab. J. Geosci.*, **7**, 5367–5381, doi: [10.1007/s12517-013-1086-z](https://doi.org/10.1007/s12517-013-1086-z).
- Nazaripour, H., and M. R. M. Daneshvar, 2014: Spatial contribution of one-day precipitations variability to rainy days and rainfall amounts in Iran. *Int. J. Environ. Sci. Technol.*, **11**, 1751–1758, doi: [10.1007/s13762-014-0616-x](https://doi.org/10.1007/s13762-014-0616-x).
- Pal, J. S., and E. A. B. Eltahir, 2016: Future temperature in southwest Asia projected to exceed a threshold for human adaptability. *Nat. Climate Change*, **6**, 197–200, doi: [10.1038/nclimate2833](https://doi.org/10.1038/nclimate2833).
- Perkins-Kirkpatrick, S. E., and P. B. Gibson, 2017: Changes in regional heatwave characteristics as a function of increasing global temperature. *Sci. Rep.*, **7**, 12256, doi: [10.1038/s41598-017-12520-2](https://doi.org/10.1038/s41598-017-12520-2).
- Pour, S. H., A. K. A. Wahab, S. Shahid, et al., 2019: Spatial pattern of the unidirectional trends in thermal bioclimatic indicators in Iran. *Sustainability*, **11**, 2287, doi: [10.3390/su11082287](https://doi.org/10.3390/su11082287).
- Právělī, R., 2016: Drylands extent and environmental issues. A global approach. *Earth-Sci. Rev.*, **161**, 259–278, doi: [10.1016/j.earscirev.2016.08.003](https://doi.org/10.1016/j.earscirev.2016.08.003).
- Qiu, X., L. J. Zhang, W. L. Li, et al., 2016: Studies on changes and cause of the minimum air temperature in Songnen Plain of China during 1961–2010. *Acta Ecol. Sinica*, **36**, 311–320, doi: [10.1016/j.chnaes.2016.06.009](https://doi.org/10.1016/j.chnaes.2016.06.009).
- Qu, M., J. Wan, and X. J. Hao, 2014: Analysis of diurnal air temperature range change in the continental United States. *Wea. Climate Extremes*, **4**, 86–95, doi: [10.1016/j.wace.2014.05.002](https://doi.org/10.1016/j.wace.2014.05.002).
- Rahimi, J., M. Ebrahimpour, and A. Khalili, 2013: Spatial changes of Extended De Martonne climatic zones affected by climate change in Iran. *Theor. Appl. Climatol.*, **112**, 409–418, doi: [10.1007/s00704-012-0741-8](https://doi.org/10.1007/s00704-012-0741-8).
- Rahimzadeh, F., A. Asgari, and E. Fattahi, 2009: Variability of extreme temperature and precipitation in Iran during recent decades. *Int. J. Climatol.*, **29**, 329–343, doi: [10.1002/joc.1739](https://doi.org/10.1002/joc.1739).
- Rahmstorf, S., G. Foster, and N. Cahill, 2017: Global temperature evolution: Recent trends and some pitfalls. *Environ. Res. Lett.*, **12**, 054001, doi: [10.1088/1748-9326/aa6825](https://doi.org/10.1088/1748-9326/aa6825).
- Rashki, A., D. G. Kaskaoutis, A. S. Goudie, et al., 2013: Dryness of ephemeral lakes and consequences for dust activity: The case of the Hamoun drainage basin, southeastern Iran. *Sci. Total Environ.*, **463–464**, 552–564, doi: [10.1016/j.scitotenv.2013.06.045](https://doi.org/10.1016/j.scitotenv.2013.06.045).
- Saboohi, R., S. Soltani, and M. Khodagholi, 2012: Trend analysis of temperature parameters in Iran. *Theor. Appl. Climatol.*, **109**, 529–547, doi: [10.1007/s00704-012-0590-5](https://doi.org/10.1007/s00704-012-0590-5).
- Shi, J., L. L. Cui, Y. Ma, et al., 2018: Trends in temperature extremes and their association with circulation patterns in China during 1961–2015. *Atmos. Res.*, **212**, 259–272, doi: [10.1016/j.atmosres.2018.05.024](https://doi.org/10.1016/j.atmosres.2018.05.024).
- Smadi, M. M., 2006: Observed abrupt changes in minimum and maximum temperatures in Jordan in the 20th century. *Amer. J. Environ. Sci.*, **2**, 114–120. Available online at <https://thes-cipub.com/abstract/10.3844/ajessp.2006.114.120>. Accessed on 30 May 2022.
- Smirnoff, H., 1939: Sur les écarts de la courbe de distribution em-

- pirique. *Rec. Math. (Mat. Sbornik)*, **6**, 3–26. Available online at http://www.mathnet.ru/php/archive.phtml?wshow=paper&jrnid=sm&paperid=5810&option_lang=eng. Accessed on 30 May 2022.
- Soltani, M., P. Laux, H. Kunstmann, et al., 2016: Assessment of climate variations in temperature and precipitation extreme events over Iran. *Theor. Appl. Climatol.*, **126**, 775–795, doi: [10.1007/s00704-015-1609-5](https://doi.org/10.1007/s00704-015-1609-5).
- Sonali, P., and D. N. Kumar, 2013: Review of trend detection methods and their application to detect temperature changes in India. *J. Hydrol.*, **476**, 212–227, doi: [10.1016/j.jhydrol.2012.10.034](https://doi.org/10.1016/j.jhydrol.2012.10.034).
- Soureshjani, H. K., A. G. Dehkordi, and M. Bahador, 2019: Temperature effect on yield of winter and spring irrigated crops. *Agric. For. Meteor.*, **279**, 107664, doi: [10.1016/j.agrformet.2019.107664](https://doi.org/10.1016/j.agrformet.2019.107664).
- Stjern, C. W., B. H. Samset, O. Boucher, et al., 2020: How aerosols and greenhouse gases influence the diurnal temperature range. *Atmos. Chem. Phys.*, **20**, 13,467–13,480, doi: [10.5194/acp-20-13467-2020](https://doi.org/10.5194/acp-20-13467-2020).
- Tabari, H., and P. H. Talaee, 2011: Analysis of trends in temperature data in arid and semi-arid regions of Iran. *Glob. Planet. Change*, **79**, 1–10, doi: [10.1016/j.gloplacha.2011.07.008](https://doi.org/10.1016/j.gloplacha.2011.07.008).
- Tabari, H., and P. Willems, 2018: Seasonally varying footprint of climate change on precipitation in the Middle East. *Sci. Rep.*, **8**, 4435, doi: [10.1038/s41598-018-22795-8](https://doi.org/10.1038/s41598-018-22795-8).
- Türkes, M., U. M. Sümer, and G. Kılıç, 1996: Observed changes in maximum and minimum temperatures in Turkey. *Int. J. Climatol.*, **16**, 463–477, doi: [10.1002/\(SICI\)1097-0088\(199604\)16:4<463::AID-JOC13>3.0.CO;2-G](https://doi.org/10.1002/(SICI)1097-0088(199604)16:4<463::AID-JOC13>3.0.CO;2-G).
- United Nations, 2019: *World Population Prospects 2019*. Department of Economic and Social Affairs Population Division, New York, 374 pp.
- Wang, P., T. C. Xie, J. G. Dai, et al., 2017: Trends and variability in precipitable water vapor throughout North China from 1979 to 2015. *Adv. Meteor.*, **2017**, 7804823, doi: [10.1155/2017/7804823](https://doi.org/10.1155/2017/7804823).
- Wang, X. Y., Y. Q. Li, Y. P. Chen, et al., 2018: Temporal and spatial variation of extreme temperatures in an agro-pastoral ecotone of northern China from 1960 to 2016. *Sci. Rep.*, **8**, 8787, doi: [10.1038/s41598-018-27066-0](https://doi.org/10.1038/s41598-018-27066-0).
- Yang, Y., M. Gao, N. R. Xie, et al., 2020: Relating anomalous large-scale atmospheric circulation patterns to temperature and precipitation anomalies in the East Asian monsoon region. *Atmos. Res.*, **232**, 104679, doi: [10.1016/j.atmosres.2019.104679](https://doi.org/10.1016/j.atmosres.2019.104679).
- You, Q. L., J. Z. Min, K. Fraedrich, et al., 2014: Projected trends in mean, maximum, and minimum surface temperature in China from simulations. *Glob. Planet. Change*, **112**, 53–63, doi: [10.1016/j.gloplacha.2013.11.006](https://doi.org/10.1016/j.gloplacha.2013.11.006).
- Yu, D. L., W. J. Li, and Y. Zhou, 2019: Analysis of trends in air temperature at Chinese stations considering the long-range correlation effect. *Phys. A: Stat. Mech. Appl.*, **533**, 122034, doi: [10.1016/j.physa.2019.122034](https://doi.org/10.1016/j.physa.2019.122034).
- Zhang, L. P., L. X. Wu, and B. L. Gan, 2013: Modes and mechanisms of global water vapor variability over the twentieth century. *J. Climate*, **26**, 5578–5593, doi: [10.1175/JCLI-D-12-00585.1](https://doi.org/10.1175/JCLI-D-12-00585.1).